

Acoustic Absorption of a New Class of Alumina Foams with Various High-Porosity Levels

Tomasz G. ZIELIŃSKI⁽¹⁾, Marek POTOCZEK⁽²⁾, Romana E. ŚLIWA⁽³⁾, Łukasz J. NOWAK⁽⁴⁾

⁽¹⁾ *Institute of Fundamental Technological Research
Polish Academy of Sciences*

Pawińskiego 5B, 02-106 Warszawa, Poland; e-mail: tzielins@ippt.pan.pl

⁽²⁾ *Faculty of Chemistry, Rzeszow University of Technology
al. Powstańców Warszawy 12, 35-959 Rzeszów, Poland*

⁽³⁾ *Faculty of Mechanical Engineering and Aeronautics, Rzeszow University of Technology
al. Powstańców Warszawy 12, 35-959 Rzeszów, Poland*

(received May 7, 2013; accepted October 2, 2013)

Recently, a new class of ceramic foams with porosity levels up to 90% has been developed as a result of the association of the gelcasting process and aeration of the ceramic suspension. This paper presents and discusses original results advertising sound absorbing capabilities of such foams. The authors manufactured three types of alumina foams in order to investigate three porosity levels, namely: 72, 88, and 90%. The microstructure of foams was examined and typical dimensions and average sizes of cells (pores) and cell-linking windows were found for each porosity case. Then, the acoustic absorption coefficient was measured in a wide frequency range for several samples of various thickness cut out from the foams. The results were discussed and compared with the acoustic absorption of typical polyurethane foams proving that the alumina foams with high porosity of 88–90% have excellent sound absorbing properties competitive with the quality of sound absorbing PU foams of higher porosity.

Keywords: sound absorption, porous materials, alumina foams.

1. Introduction

Sound absorptivity of porous media is determined by its total and open porosity, flow resistivity, tortuosity, characteristic sizes of pores and windows linking the pores. In the case of soft materials – like polyurethane (PU) foams – the elasticity of skeleton plays an important role in the lower frequency range. Although PU foams are lightweight materials and some of them have excellent sound absorbing and insulating properties, they cannot be used in many applications, especially, under extreme conditions such as high temperatures, high intensity sound and velocity flow of air, oil contamination and humidification – in such applications (for example, as a material for acoustical liner in turbofan engines) metal foams (BO, TIANNING, 2009) or ceramic foams are adequate.

Ceramic foams are light-weight materials with unique properties such as low density, low thermal conductivity, low dielectric constant, low thermal mass,

high specific strength, high permeability, high thermal shock resistance, high porosity, high specific surface area, high resistance to chemical corrosion, making them indispensable for various engineering applications (COLOMBO, 2006; GREEN, COLOMBO, 2003). These materials are being considered for a whole range of potential aerospace applications, including sound absorbers, thermal insulation, and light-weight structures.

It is well known that many of the above mentioned parameters (like porosity, flow resistivity, pore dimensions, etc.) may be controlled during the production processes in ceramics, and their effects on sound absorption capability of porous ceramics should therefore be studied. Thus, for example, TAKAHARA (1994) investigated sound absorption of porous ceramic material $\text{Al}_2\text{O}_3\text{-SiO}_2$ with porosity from 49 to 55% (although most of the presented results are for the highest value of 55%). For samples with 55% porosity he determined and compared sound absorption with respect

to the sample thickness, namely, 50 mm or 10 mm. In the case of the 50 mm thick sample the absorption coefficient exceeded 0.6 at frequencies above 500 Hz. For the 10 mm thick sample the absorption was much inferior – it exceeded 0.4 above 1 kHz; to improve it an air gap may be added between the sample and the reverberant enclosure (rigid wall). Therefore, the influence of such backing cavity of 85 mm depth on the absorption of the combined (95 mm thick) system of porous ceramic layer and air gap was also shown. For 50 mm thick samples the effect of flow resistivity and porosity was illustrated by comparing results obtained for three different values of these parameters. Sound insulating characteristics of porous ceramics $\text{Al}_2\text{O}_3\text{-SiO}_2$ were also investigated by TAKAHARA (1982) in his earlier work where he presented transmission loss and absorption coefficient for 25 mm-thick sample of porous ceramics with 55% porosity.

Effects of surfactants on some intrinsic properties of porous building ceramics were investigated by FUJI *et al.* (2006). They measured the sound absorption coefficient in the frequency range from 0.5 to 6.5 kHz for porous ceramics fabricated by gelcasting using different surfactants, namely: (a) ammonium lauryl sulphate, (b) fatty alcohol ethoxy sodium, and (c) poly-(oxyethylene)-sorbitan monolaurate. The best results were achieved for the first two surfactants, however, they seem to be rather mediocre when comparing with typical PU foams (although this cannot be clearly stated, since unfortunately, the thickness of ceramic samples is not given). The acoustic absorption coefficient is app. 0.3 at lower frequencies, exceeding 0.4 in the higher frequency range, reaching 0.5 in the case of ammonium lauryl sulphate. For this surfactant the absorption is the best and the total porosity of porous ceramics is 64.7%, whereas the open porosity is 53.4%; in the case when the alcohol ethoxy sodium was used they are 52.3% and 38.6%, respectively. In another work (ZHANG *et al.*, 2006) the authors show that the acoustic absorption can be improved when the porous ceramics is fabricated by gelcasting using a continuous process. By this new method a better pore size distribution is achieved, which improves the total and open porosities (to 68.3% and 73.5%, respectively), and that has its effect on the acoustic absorption which now exceeds 0.5 at 3.3 kHz, reaching 0.7 at 6.4 kHz.

GIESE *et al.* (2011) presented a new processing technique – combining the freeze gelation process with sacrificial templating – to create porous sound absorption ceramics for high-temperature applications. The process leads to near-net shape components with open-cell porosity which can be increased up to 74% by adding expanded perlite as melting filler. Sound absorption was measured in the frequency range from 250 to 1400 Hz for three samples made up of ceramics with different open porosity, namely, 74, 73, and 67%, and various corresponding flow resistance; each of the sam-

ples had the same thickness of 30 mm. The absorption results were very good for two samples of higher porosities, exceeding 0.4 at frequencies above 200 Hz (the maximum value for the sample with porosity 74% was above 0.6 at app. 400 Hz), however, the configuration involved a 50 mm air gap behind the sample, which generally increases the frequency range with a high absorption coefficient towards lower frequencies (notice that the total thickness to the reverberant enclosure was 70 mm); therefore, these results cannot be directly compared with standard tests performed with no gap.

Sound absorption capabilities of porous zeolite with macropores – which is a ceramic material fabricated by high-temperature sintering – were recently investigated by CUIYUN *et al.* (2012). They measured acoustic absorption coefficient in the frequency range from 200 Hz to 4 kHz for 8 ceramic samples with various porosity, bulk density, flow resistivity, and thickness. For three samples the porosity was 60%, for another three it was app. 70%, for one sample it was 64%, and it was 76% for yet another one. The mean pore size varied from 1.1 to 2.9 mm, while it was 6.2 mm for one sample. The sample thickness was: 15, 20, 25, or 28 mm. The measurements showed excellent sound absorbing properties of this ceramics: for most of the samples the acoustic absorption exceeded 0.7 at frequencies over 1.5 kHz, often with some peak/maximum value exceeding 0.9 at 2 or 2.5 kHz. Two analytical models – a simple two-parameter model by Delany and Bazley, and more advanced Johnson-Allard model (ALLARD, ATALLA, 2009), were applied to calculate the absorption coefficient. The latter one showed a better fit to the experimental results, however, the analytical curves were in general very approximative: they were very smooth (the Delany-Bazley curves were even nearly monotonic) and no characteristic peaks were represented.

Corrundum materials have been subject to some acoustical measurements, like acoustic emission (see, for example, RANACHOWSKI *et al.* (2009)) or sound absorption (see some references above), however, in the case of the corrundum or other ceramic foams their porosity was always significantly inferior than the porosity of the recently developed corrundum foam tested in the present paper. It will be shown below that this high porosity ratio together with some microstructural features described in this paper (like typical size of pores and windows linking the pores) contribute to the excellent acoustical properties comparable only with the best of PU foams.

2. Characterization of a new class of alumina foams

In recent years, a new class of ceramic foams with porosity levels up to 90% has been developed as a re-

sult of the association of the gelcasting process and aeration of the ceramic suspension containing foaming agents and gelling agents (SEPULVEDA, BINNER, 1999; SEPULVEDA, 1997). The in situ polymerisation of gelling agents, led to fast solidification, resulting in strong porous bodies. The next step is calcination followed by sintering at high temperature.

Ceramic suspensions of alumina powder (CT 3000 SG, Alcoa Chemie, Ludwigshafen, Germany) were prepared to a solid loading of 55 vol.% by dispersing them with 0.5 wt.% of dispersant (Darvan 821A, R.T. Vanderbilt, U.S.A.). Next, the agarose solution as a gelling agent was added to the slurry maintaining the temperature of all constituents at 60°C. Foaming was conducted through agitation, with the help of a double-blade mixer at 60°C. Addition of non-ionic surfactants (Tergitol TMN-10, Aldrich, Germany) was necessary to stabilise the foam. Gelation was performed by cooling the foam to 15°C. The green body was then de-molded and left in room conditions to dry. Sintering was performed at 1575°C for 2 hours. The details are described in the paper by POCZEK (2008). The Al₂O₃ foams were manufactured in that way in the form of cylinders of various height (thickness; see below) in three main cases of porosity levels, namely: 72%, 88%, and 90% (also 89.5%). Ceramic samples were cut out from the cylinders and served for acoustic measurements described in the next Sections.

The density of porous bodies was calculated from the mass and dimensions of a minimum of five samples with regular shapes. The theoretical density of fully densified alumina (3.98 g/cm³) was used as a reference to calculate the total volume fraction of porosity. The microstructure of ceramic foams was observed by scanning electron microscopy (SEM), (Jeol JSM-5500 LV). The fractured samples first were coated with a thin layer of gold. Pictures for monitoring the cellular structure were taken for estimation of cell and window sizes. This allowed window and cell size to be estimated from cells which presented an equator in the fracture surface and from windows by taking the major axis of oblique windows as the true diameter. The diameter of minimum 150 cells and 350 windows was measured for each sample and the pore and window size distributions were calculated.

The densities of alumina foams were found to be between 0.40 and 1.11 g/cm³, and the calculated total porosity varied between 90 and 72%, respectively. It is important to notice that the foam porosity is strongly related to the typical microstructural sizes, like, for example, their pore (or cell) diameters. The microstructure of the sintered foams is presented in Fig. 1 for the three considered cases of porosity, namely: 90, 88, and 72%. The alumina foams are typically composed of approximately spherical cells interconnected by circular windows. The cell size and the window size decrease

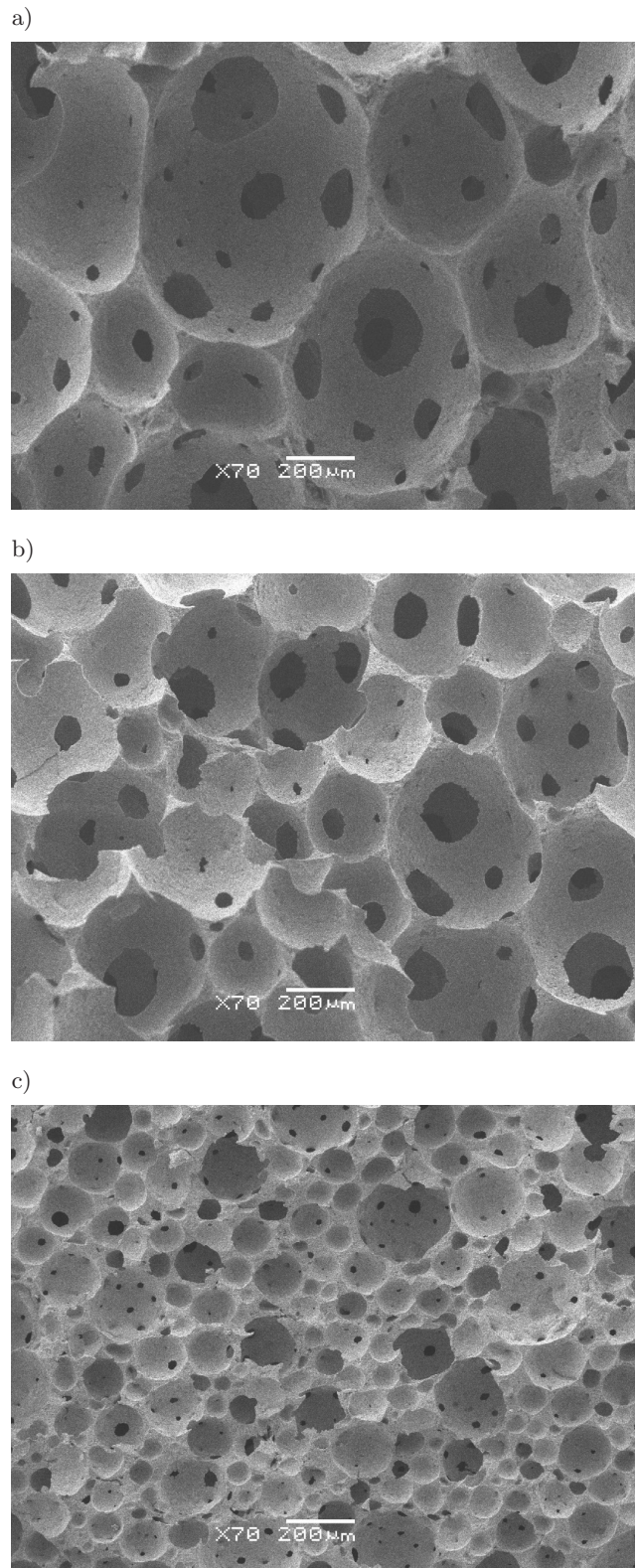


Fig. 1. SEM cross-section of alumina foams having porosity of: a) 90%, b) 88%, and c) 72%.

with increasing of porosity in alumina foams. This is illustrated in Figs. 2 and 3 where the cumulative fractions of cell and window diameters are shown for the

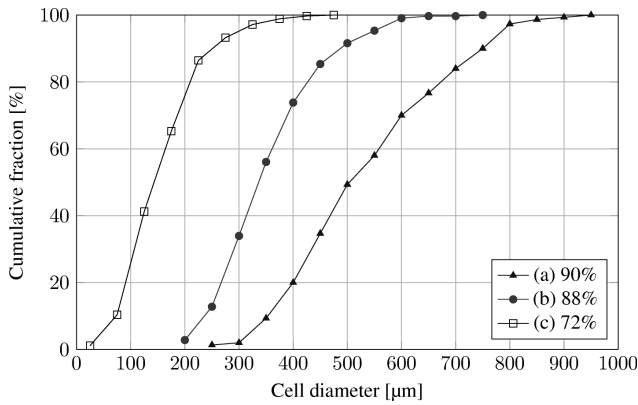


Fig. 2. Cumulative fraction of cell diameters of alumina foams with porosity of: a) 90%, b) 88%, and c) 72%.

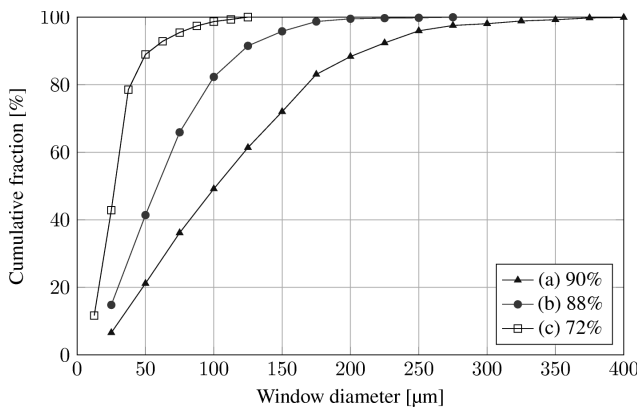


Fig. 3. Cumulative fraction of window diameters of alumina foams with porosity of: a) 90%, b) 88%, and c) 72%.

three cases of porosity. Table 1 provides the median value of cell and window sizes for these three types of alumina foam.

Table 1. Average diameters of cells and windows for alumina foams with particular porosity.

Porosity [%]	Average diameter [μm]	
	of cells	of windows
90	505	101
88	380	60
72	135	28

3. Acoustical testing

All acoustical measurements of ceramic samples were performed using the so-called transfer function method (see, for example, CHUNG, BLASER (1980); DALMONT (2001); BOONEN, SAS (2004)) according to the ISO 10534-2 standard (ISO, 1998). To this end two-microphone configuration of impedance tube was used – the whole experimental setup is shown in Fig. 4. A sample is set at the rigid-wall termination (or, sometimes, leaving an air gap of known thickness, between

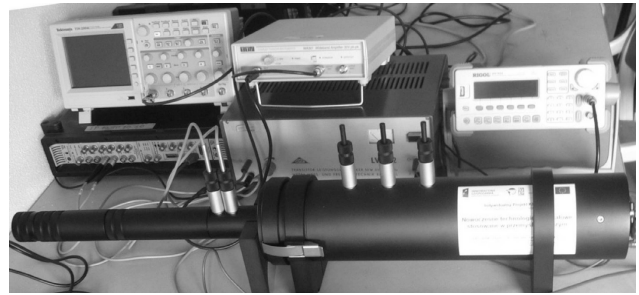


Fig. 4. Experimental setup for measurement of acoustic absorption coefficient of materials.

the wall and the sample) at one end in the impedance tube. At the other end, a loudspeaker is mounted which is driven by a broadband, stationary random signal to generate plane acoustic waves which arrive at the sample, penetrate it, and are reflected by the wall. A standing-wave interference pattern results due to the superposition of forward and backward-travelling waves inside the tube. Basing on measurements of the sound pressure at two fixed locations, the so-called complex transfer function is calculated, which can be used to determine acoustical properties of the sample, namely: the normal acoustic impedance, the complex reflection coefficient, and the sound absorption coefficient. Operating frequency range of the instrument depends on the spacing between the microphone positions and on the sample size. The correctness and accuracy of the method strongly depend on the calibration of microphones, which requires measurements of the transfer function for two configurations of the microphones, in their normal and interchanged positions. If the improved calibration procedure proposed by BOONEN, SAS (2004) is used the temperature and ambient pressure measurements are superfluous since then the exact estimation of the actual speed of sound in air is not necessary.

Sound absorption capability was determined for corundum ceramic foams with various porosity, namely: 90%, 88%, 72%, and again also for 89.5%. For each of these porosities two samples were manufactured in the form of cylinders with 29 mm diameter and various thickness (height), see Fig. 5; the cor-



Fig. 5. Ceramic samples prepared for measurements in the impedance tube with diameter 29 mm; the samples 5 and 6 are made up with plaster, whereas the samples 7 and 8 are wrapped up in a thin tape in order to fit well in the tube.

responding data for all samples are given in Table 2. For such sample diameter the valid frequency range for measurements in the impedance tube was from 500 Hz to 6.4 kHz.

All samples with porosity 90% or 88% fitted very well in the measurement tube, while the lateral surfaces of samples with porosity 72% were additionally made up with plaster, and the samples with porosity 89.5% were wrapped up in a thin (transparent) tape in order to fit well. Nevertheless, the fitting was done accordingly to the standard procedure and it should not affect the testing results.

Table 2. Porosity and thickness of cylindrical samples of ceramics Al_2O_3 .

No.	Label	Porosity [%]	Thickness [mm]
1	p90h18	90	18
2	p90h24	90	24
3	p88h14	88	14
4	p88h17	88	16.5
5	p72h16	72	16
6	p72h22	72	22
7	p89h18	89.5	18
8	p89h22	89.5	22

4. Discussion of the results

Figures 6, 7, and 8 show the curves of the acoustic absorption coefficient determined for ceramic samples with porosity 90%, 88%, and 72%, respectively. Additionally, on each of these graphs absorption curves for typical polyurethane (PU) foams are shown for com-

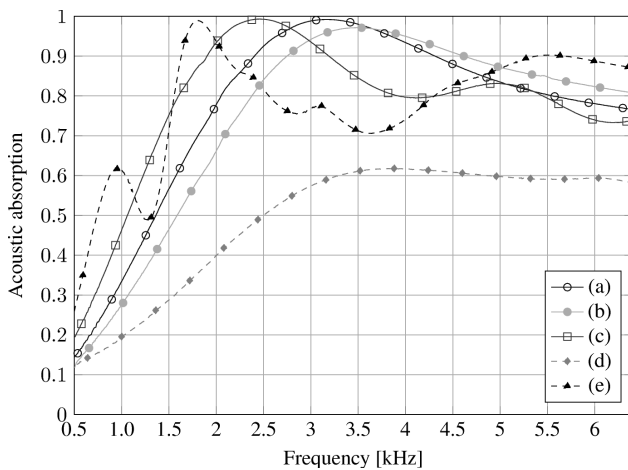


Fig. 6. Acoustic absorption of ceramic samples with porosity 90%: (a, b) thickness 18 mm, face 'A' and 'B', (c) thickness 24 mm. Acoustic absorption of PU foams with porosity app. 98%: (d) stiff PU foam, thickness 26 mm, (e) soft PU foam, thickness 21 mm.

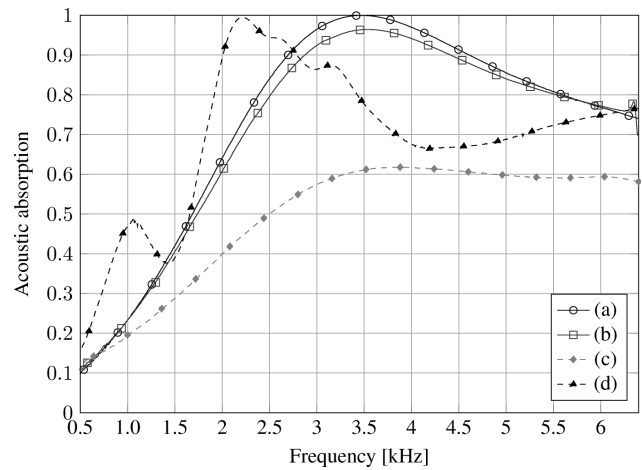


Fig. 7. Acoustic absorption of ceramic samples with porosity 88%: (a) thickness 14 mm, (b) thickness 16.5 mm. Acoustic absorption of PU foams with porosity app. 98%: (c) stiff PU foam, thickness 26 mm, (d) soft PU foam, thickness 16 mm.

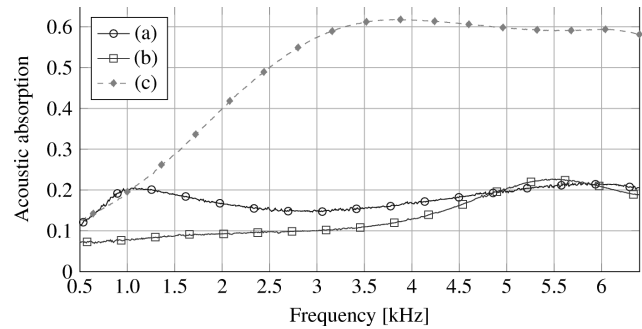


Fig. 8. Acoustic absorption of ceramic samples with porosity 72%: (a) thickness 16 mm, (b) thickness 22 mm. Acoustic absorption of stiff PU foam with porosity app. 98%: (c) thickness 26 mm.

parison. The porosity of PU foams was approximately 98% (as declared by the producer) and the thickness of samples was taken to be in some correspondence with the thickness of relevant ceramic samples. All acoustical measurements were carried out for both sides (faces) of all porous samples. In general, the opposite-side measurements were (nearly) identical, because of the macroscopic homogeneity of the examined porous materials; thus, instead of showing two almost overlapping curves only one of them (or the average result) is presented. The both opposite-side absorption curves are shown only for one sample p90h18 – see curves (a) and (b) in Fig. 6 – those curves do not overlap and are slightly different because of some distinct imperfections on one of the sample faces (curve (b), face 'B').

One should observe that the acoustic absorption is very good for ceramic samples with open-cell porosity of 90% and 88% (Figs. 6 and 7, respectively),

while it is poor for ceramics with closed-cell porosity of 72% (see Fig. 8). Results for the open-cell ceramic foams should be compared with acoustic absorption of typical polyurethane foams which are considered very good sound absorbing and insulating materials. From Fig. 6 one can see that the acoustic absorption of ceramic samples with porosity 90% (and thickness 18 mm or 24 mm) is comparable with the absorption of soft PU foam – thickness 21 mm, curve (e) in Fig. 6; in some frequency ranges it is even superior. Notice that at lower frequencies (app. at 0.9 kHz and 1.8 kHz) acoustic resonances resulting from the motion of elastic skeleton of the soft PU foam are visible; at higher frequencies the skeleton behaviour tends to be rigid even for the soft PU foam. This is a typical situation for soft PU foams: the low-frequency resonances and anti-resonances of elastic skeleton significantly influence sound propagation and absorption; the flexibility of elastic skeleton may also be utilized in order to improve the acoustic absorption in semi-active (ZIELINSKI, RAK, 2010) or active way (ZIELINSKI, 2008; 2010; 2011). The sound absorption properties of PU foams may also be improved passively by changing the skeleton density and stiffness – this can be attained by adding some inclusions in the foam matrix, for example, rice hull (WANG *et al.*, 2013), or tea-leaf-fibres (EKICI, 2012). The acoustic absorption curve for a stiff PU foam – thickness 26 mm, curve (d) in Fig. 6 – does not manifest any skeleton resonances and is inferior in the whole frequency range. Similar conclusions can be drawn when comparing the acoustic absorption of ceramic samples of 88% porosity with the absorption of soft and stiff PU foams. Apart from some lower frequency resonances, the sound absorption performance for a 16 mm high sample of soft PU foam – illustrated by the absorption curve (c) in Fig. 7 – tend to be comparable with the absorption performance obtained for ceramic samples of similar thickness; however, it is distinctly superior around the elastic skeleton resonances at 1.1 kHz and 2.2 kHz. The absorption coefficient for the stiff PU foam – curve (c) in Fig. 7 – is inferior in the whole frequency range.

It is important to notice that changes between the absorption curves obtained for ceramic samples of the same porosity but different thickness result mainly (if not only) from that difference in thickness, and not from some subtle local variations in morphology which can be neglected on the macroscopic scale, especially at lower frequencies. For example, notice that the absorption curves (a) and (b) from Fig. 7 are fairly similar since the thickness difference between these samples with porosity 88% is not significant. This observation is also confirmed in Fig. 9, where absorption curves are presented for all ceramic samples, and additionally, for samples with 89.5% porosity: notice that absorption coefficients measured for samples p90h18

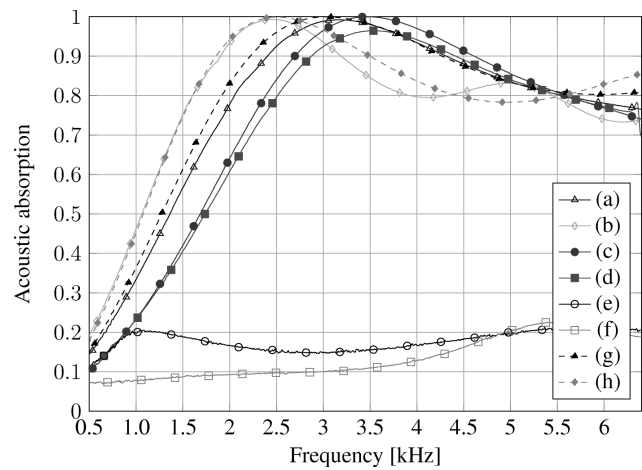


Fig. 9. Acoustic absorption of Al_2O_3 ceramic samples with porosity: (a,b) 90%, (c,d) 88%, (e,f) 72%, (g,h) 89.5%; and thickness: (a) 18 mm, (b) 24 mm, (c) 14 mm, (d) 16.5 mm, (e) 16 mm, (f) 22 mm, (g) 18 mm, (h) 22 mm.

and p89h18, namely, curves (a) and (g) in Fig. 9, are very similar (and, as a matter of fact, identical in the lower frequency range) since the samples have exactly the same thickness (18 mm) and nearly identical porosity (90% and 89.5%, respectively); similarly, the results obtained for samples p90h24 and p89h22 – curves (b) and (h) in Fig. 9 – are also very close to each other, since the samples have similar thickness (24 mm and 22 mm) and nearly identical porosity (90% and 89.5%, respectively). All this shows that alumina foams are manufactured with repeatable micro-morphology, and moreover, they are macroscopically homogeneous and for a given porosity should manifest typical values of average macroscopic parameters relevant for sound propagation, like permeability or tortuosity.

5. Conclusions

- The microstructure of alumina foams is typically composed of approximately spherical cells interconnected by circular windows. Depending on the porosity (72–90%) the median cell size ranged from 135 to 505 μm , while the median window size varied from 28 to 101 μm .
- Such foams are highly porous ceramics. In case of fully open-cell porosity of 88–90% the alumina foams exhibit excellent sound absorbing properties comparable with the best sound insulating polyurethane foams.
- The repeatability of results obtained for samples cut out from foams (with the porosity of app. 90%) produced at different times shows that alumina foams are manufactured with recurrent micro-morphology which is correlated with the parameter of the total

porosity. They can be considered as macroscopically homogeneous and isotropic.

- A typical character of the frequency-dependent curves of the acoustic absorption coefficient confirms that (from the modelling perspective) they can be treated as porous media with rigid skeleton. These curves may be utilised for some parametric estimation, for example, using procedures for inverse identification of parameters for sound absorption modelling of porous ceramics and other rigid porous media proposed recently by ZIELINSKI (2012).

Acknowledgments

Financial support of Structural Funds in the Operational Programme – Innovative Economy (IE OP), financed from the European Regional Development Fund – Project “Modern Material Technologies in Aerospace Industry”, No. POIG.0101.02-00-015/08, is gratefully acknowledged. Mr. Nowak also would like to acknowledge the financial support of the National Science Centre (NCN) within the framework of his PhD project No. UMO-2011/01/N/ST8/07755.

References

1. ALLARD J.F., ATALLA N. (2009), *Propagation of Sound in Porous Media: Modelling Sound Absorbing Materials*, Second Edition, Wiley.
2. BO Z., TIANNING C. (2009), *Calculation of sound absorption characteristics of porous sintered fiber metal*, Appl. Acoust., **70**, 337–346.
3. BOONEN R., SAS P. (2004), *Calibration of the two microphone transfer function method to measure acoustical impedance in a wide frequency range*, Proceedings of ISMA 2004: International Conference on Noise and Vibration Engineering, SAS P., DEMUNCK M. [Eds.], Leuven (Belgium), 325–336.
4. CHUNG J.Y., BLASER D. (1980), *Transfer function method of measuring in-duct acoustic properties*, J. Acoust. Soc. Am., **68**, 3, 907–921.
5. COLOMBO P. (2006), *Conventional and novel processing for cellular ceramics*, Philosophical Transaction of the Royal Society A, **364**, 109–124.
6. CUIYUN D., GUANG C., XINBANG X., PEISHENG L. (2012), *Sound absorption characteristics of a high-temperature sintering porous ceramic material*, Appl. Acoust., **73**, 865–871.
7. DALMONT J.-P. (2001), *Acoustic impedance measurement, Part I: A review. Part II: A new calibration method*, J. Sound Vib., **243**, 3, 427–459.
8. EKICI B., KENTLI A., KÜÇÜK H. (2012), *Improving sound absorption property of polyurethane foams by adding tea-leaf fibers*, Archives of Acoustics, **37**, 4, 515–520.
9. FUJI M., KATO T., ZHANG F.-Z., TAKAHASHI M. (2006), *Effects of surfactants on the microstructure and some intrinsic properties of porous building ceramics fabricated by gelcasting*, Ceram. Int., **32**, 797–802.
10. GIESE F., EIGENBROD C., KOCH D. (2011), *A novel production method for porous sound-absorbing ceramic material for high-temperature applications*, Int. J. Appl. Ceram. Technol., **8**, 3, 646–652.
11. GREEN D.J., COLOMBO P. (2003), *Cellular ceramics: intriguing structures, novel properties, and innovative applications*, Materials Research Bulletin, **28**, 296–300.
12. ISO 10534-2 (1998), *Determination of sound absorption coefficient and impedance in impedance tubes*, International Standard Organisation.
13. POTOCZEK M. (2008), *Gelcasting of alumina foams using agarose solutions*, Ceramics International, **34**, 661–667.
14. RANACHOWSKI P., REJMUND F., RANACHOWSKI Z., PAWELEK A., PIATKOWSKI A. (2009), *Comparison of acoustic emission and structure degradation in compressed porcelain and corundum materias*, Archives of Acoustics, **34**, 4, 655–676.
15. SEPULVEDA P. (1997), *Gelcasting of foams for porous ceramics*, American Ceramic Society Bulletin, **76**, 61–65.
16. SEPULVEDA P., BINNER J.G.P. (1999), *Processing of cellular ceramics by foaming and in situ polymerisation of organic monomers*, Journal European Ceramic Society, **19**, 2059–2066.
17. TAKAHARA H. (1982), *Sound insulating characteristics of porous ceramic Al₂O₃-SiO₂*, Appl. Acoust., **15**, 2, 111–116.
18. TAKAHARA H. (1994), *The sound absorption characteristics of particulate porous ceramic materials*, Appl. Acoust., **41**, 3, 265–274.
19. WANG Y., ZHANG C., REN L., ICHCHOU M., GALLAND M.-A., BAREILLE O. (2013), *Influences of rice hull in polyurethane foam on its sound absorption characteristics*, Polymer Composites, article in press, published online in Wiley Online Library, doi:10.1002/pc.22590.
20. ZHANG F.-Z., KATO T., FUJI M., TAKAHASHI M. (2006), *Gelcasting fabrication of porous ceramics using a continuous process*, J. Eur. Ceram. Soc., **26**, 667–671.
21. ZIELINSKI T.G. (2008), *Active porous composites for wide frequency-range noise absorption*, Proceedings of ISMA2008: International Conference on Sound and Vibration, Leuven (Belgium), 89–103.
22. ZIELINSKI T.G. (2010), *Fundamentals of multiphysics modelling of piezo-poro-elastic structures*, Archives of Mechanics, **62**, 5, 343–378.

23. ZIELINSKI T.G. (2011), *Numerical investigation of active porous composites with enhanced acoustic absorption*, Journal of Sound and Vibration, **330**, 5292–5308.
24. ZIELINSKI T.G. (2012), *Inverse identification and microscopic estimation of parameters for models of sound absorption in porous ceramics*, Proceedings of International Conference on Noise and Vibration Engineering (ISMA2012)/International Conference on Uncertainty in Structural Dynamics (USD2012), SAS P., MOENS D., JONCKHEERE S. [Eds.], Leuven (Belgium), 95–107.
25. ZIELINSKI T.G., RAK M. (2010), *Acoustic absorption of foams coated with MR fluid under the influence of magnetic field*, J. Intell. Mater. Syst. Struct., **21**, 125–131.